Membrane Water Treatment, *Vol. 6, No. 2 (2015) 127-139*
DOI: http://dx.doi.org/10.12989/mwt.2015.6.2.127

Inverse HPLC approach for the evaluation of repulsive interaction between ionic solutes and a membrane polymer

Yoshiaki Kiso [1], Yuki Kamimoto [2], Katsuya Hosogi [1] and Yong-Jun Jung [*3]

[1] *Department of Environmental and Life Sciences, Toyohashi University of Technology, Tempaku-cho, Toyohashi 441-8586, Japan*
[2] *EcoTopia Science Institute, Nagoya University, Furo-cho, Chikusa-ku, Nagoya, Aichi 464-8603, Japan*
[3] *Department of Environmental engineering, Catholic University of Pusan, Oryundae-ro, Geumjeong-gu, Busan, 609-757, Korea*

(*Received January 08, 2014, Revised December 22, 2014, Accepted February 28, 2015*)

Abstract. Rejection of ionic solutes by reverse osmosis (RO) and nanofiltration (NF) membranes is controlled mainly by electrochemical interaction as well as pore size, but it is very difficult to directly evaluate such electrochemical interaction. In this work, we used an inverse HPLC method to investigate the interaction between ionic solutes and poly (*m*- phenylenediaminetrimesoyl) (PPT), a polymer similar to the skin layer of polyamide RO and NF membranes. Silica gel particles coated with PPT were used as the stationary phase, and aqueous solutions of the ionic solutes were used as the mobile phase. Chromatographs obtained for the ionic solutes showed features typical of exclusion chromatographs: the ionic solutes were eluted faster than water (mobile phase), and the exclusion intensity of the ionic solute decreased with increasing solute concentration, asymptotically approaching a minimum value. The charge density of PPT was estimated to be ca. 0.007 mol/L. On the basis of minimum exclusion intensity, the exclusion distances between a salt and neutralized PPT was examined, and the following average values were obtained: 0.49 nm for 1:1 salts, 0.57 nm for 2:1 salts, 0.60 nm for 1:2 salts, and 0.66 nm for 2:2 salts. However, $NaAsO_2$ and H_3BO_3, which are dissolved at neutral pH in their undissociated forms, were not excluded.

Keywords: reverse osmosis; nanofiltration; polyamide; ionic solute; electrochemical interaction; HPLC

1. Introduction

Membrane filtration processes such as reverse osmosis (RO) and nanofiltration (NF) are often used for water treatment processes such as desalination, softening, and removal of hazardous organic micropollutants (Ghaffour *et al*. 2013, Bruggen *et al*. 2003, Plakas and Karabelas 2012, Dolar *et al*. 2012). In such processes, solute separation is controlled by the sieving effect and by the interaction between solute and membrane material. The sieving effect is controlled by both solute size and pore radius, and the latter property is evaluated by a numerical simulation using hydrophilic organic compounds as a probe solute (Wang *et al*. 1995, 1997, Kiso *et al*. 2011). For ionic solutes, electrochemical interactions (including Donnan equilibrium) are another major

*Corresponding author, Professor, E-mail: yjjung@cup.ac.kr

http://www.techno-press.org/?journal=mwt&subpage=7 ISSN: 2005-8624 (Print), 2092-7037 (Online)

factor that controls the sieving effect, and thus electrochemical interactions should be incorporated into numerical simulations to evaluate salt rejection performance (Wang *et al*. 1997, Bowen and Welfoot 2002a, 2002b, Szymczyk and Fievet 2005, Bellona and Drewes 2005, Verliefde *et al*. 2008, Déon *et al*. 2009, Yaroshchuk 2001). In current numerical simulation models, however, the charge density of the membrane is incorporated only as a tuning parameter, because direct measurement of charge density is difficult to achieve (Schaep and Vandecasteele 2001). Direct measurement of the interaction between hydrophobic organic compounds and a membrane is also difficult, although the effects of the adsorption on rejection have been examined widely (Kiso *et al*. 2001a, b, Jung *et al*. 2005, Kimura *et al*. 2003a, b, Comerton *et al*. 2007, Semião and Schäfer 2013).

However, we have developed a useful approach to examine the interaction between organic compounds and membrane polymer (Kiso 1986, Kiso and Kitao 1989, Kiso *et al*. 1999a, b), where membrane polymer was used as a stationary phase of the high performance liquid chromatography (HPLC) system and the retention properties were measured. In our previous work (Kiso *et al*. 2014), it was also developed to use poly (*m*-phenylenediaminetrimerosoyl) (PPT: typical material of polyamide membrane) as a stationary phase, where PPT was coated on the silica particles by surface polymerization.

Considering that the inverse HPLC method gave the repulsion intensity between salt and cellulose acetate in aqueous phase (Kiso 1986), this method using the column packed with the silica particles coated with PPT may also give useful information on the electrochemical interaction between ionic solute and PPT. In this study, almost salts were excluded from the PPT surface, and the effects of slat concentration at the surface of PPT on the exclusion intensity. The effects of valence of cation and anion were also examined, and finally the charge density of PPT and the adjacent distance of a salt to the PPT surface were also discussed.

2. Materials and methods

2.1 Column packing material

The packing material used in this study consisted of silica particles coated with PPT, which was the same to the packing material used in our previous work (Kiso *et al*. 2014). The PPT thin film was prepared on the silica particles (5 μm) by surface polymerizaition with aqueous *m*-phenylenediamine solution (2% (w/v)), and an *n*-hexane solution of trimesoyl chloride (0.1% (w/v)). The specific surface area of the particles, measured by the Brunauer–Emmett–Teller method, was 253 m^2/g. The particles were packed into an HPLC column (4.6 mm i.d. × 250 mm long), and two columns connected series were used in this work. The columns packed with The zeta-potential of PPT-coated particles was measured by an ELS-Z2 (Otsuka Electronics Co., Ltd., Osaka, Japan).

The surface characterization of the PPT coated silica particle was conducted by a scanning electron microscopy and by a FT-IR, and an ignition loss of the particles was also conducted. The results obtained these analysis did not indicate difference from those of the original silica particles. However, the retention properties of the PPT coated silica particles for hydrophobic organic compounds indicated typical feature of reverse phase chromatograph as shown in our previous paper. Therefore, PPT may be coated as very thin film on the silica particle.

2.2 Inorganic salts

Table 1 List of inorganic salts and adjusted retention times

1:1		2:1		1:2 and 2:2	
salt	t_R'	salt	t_R'	salt	t_R'
LiCl	-1.02	$MgCl_2$	-0.87	K_2SO_4	-0.94
NaCl	-1.11	$CaCl_2$	-1.15	K_2CrO_4	-1.25
KCl	-0.75	$BaCl_2$	-1.06	K_2HPO_4	-1.12
RbCl	-0.85	$CoCl_2$	-1.15	$MgSO_4$	-1.27
NH_4Cl	-0.85	$MnCl_2$	-1.00	$MnSO_4$	-1.17
KBr	-0.97			$CoSO_4$	-1.31
KI	-0.82			$CuSO_4$	-1.17
KNO_3	-0.79			$ZnSO_4$	-1.19
Average	-0.894	Average	-1.046	Average	-1.177
SD*	0.125	SD*	0.117	SD*	0.113

*: standard deviation

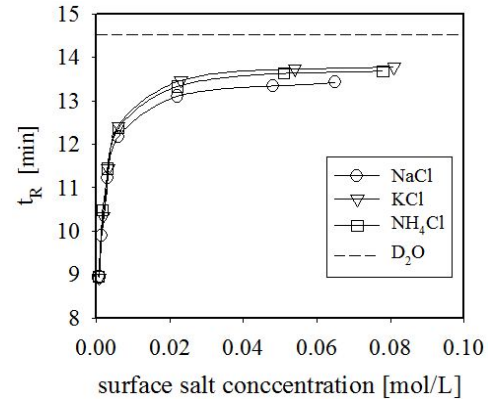

(a)

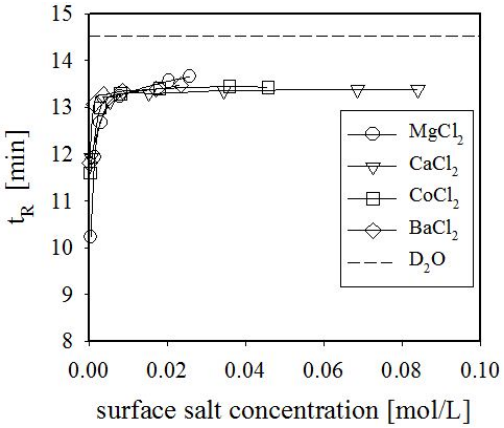

(b)

Fig. 1 (a) Plots of retention time of 1:1 salts and surface concentration at stationary phase; (b) Plots of retention time of 2:1 salts and surface concentration at stationary phase

The inorganic salts used in this work are summarized in Table 1. Each salt was dissolved in distilled-deionized water. The salt concentrations injected into the column were varied in the range from 0.01 to 1.0 mol/L.

2.3 HPLC measurement

The HPLC system consisted of a pump (PU-2080Plus, Jasco, Tokyo, Japan), a degasser (DG-2080-53, Jasco), a sample injector (20 μL, Rheodyne 7125, USA), a column oven (Co-2060Plus, Jasco), and a refractive index detector (830-RI, Jasco). HPLC data were analyzed by data processing software (ChromNAV, Jasco). Two columns packed with PPT-coated silica particles were installed in series. Distilled-deionized water was used as the mobile phase, and the flow rate was maintained at 0.5 mL/min. The column temperature was controlled at 15, 22, 30, or 40°C.

The retention property of each salt was examined on the basis of the adjusted retention time (t_R') defined as the following equation

$$t_R' = t_R - t_0 \tag{1}$$

where t_R and t_0 are retention times of a salt and an unretained compound (D_2O), respectively.

The salt concentration at the surface of the stationary phase (based on the peak intensity of the chromatogram) was evaluated from calibration curves obtained by the following procedure: the PPT columns were eliminated, a large volume injection loop (500 μL) was equipped in the system, the salt solution at concentrations ranging from 0.0005 mmol/L to 0.1 mol/L was injected, the intensity of the signal at the plateau in the chromatogram was measured, and the signal intensity was correlated with the salt concentration. The concentrations at the surface of the stationary phase were 2%-10% of the concentrations of the injected solution.

3. Results and discussion

3.1 Effect of salt concentration on retention

All salts were eluted earlier than D_2O for the entire range of salt concentrations tested, and thus negative adjusted retention times (t_R') were obtained (Table 1). Fig. 1 shows some examples of the relationship between the retention time (t_R) and the salt concentration at the surface of the stationary phase. The results shown in Fig. 1 are the typical features of exclusion chromatographs. The intensity of the exclusion (i.e., the value of t_R') was influenced by the concentration of salt: the retention times increased with increasing salt concentration and asymptotically approached a plateau. These results agree with the previously reported finding that chloride rejection decreases with increasing chloride concentration (Malaisamy *et al*. 2011).

The retention times observed at the highest concentration of each salt were assumed to be the maximum retention times, and the minimum adjusted retention times ($t_R' = t_R - t_0$) for all salts are also reported in Table 1. The average value and standard deviation of t_R' for each group of 1:1 salts, 2:1 salts, and (1:2 and 2:2) salts are reported in the bottom row of Table 1. Student's t-test (significance level: 5%) revealed that the average values for these groups differ significantly, although the standard deviations were rather large. The results indicate that the salts were excluded with increasing strength in the following order: (1:1) < (2:1) < (1:2 and 2:2). The fact that divalent

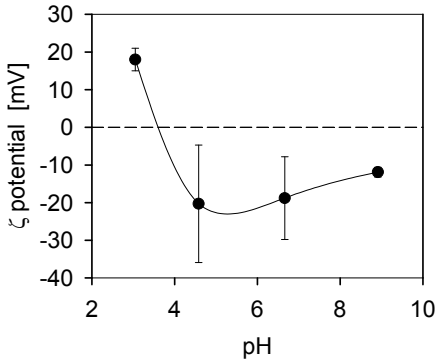

Fig. 2 ζ potential of silica particles coated with PPT

anions were excluded more strongly than divalent cations suggests that the PPT surface was charged negatively. This result is supported by the profile of potential of the packed material (Fig. 2): although the pH varied widely, the particle was charged negatively at pH 4-9.

Considering that the retention time asymptotically approached a plateau, we estimated the salt concentrations needed to saturate the surface charge of the PPT using plots of retention time versus surface salt concentration. The surface charge of PPT was saturated at ca. 0.050 mol/L for 1:1 salts; at ca. 0.035 mol/L for 1:2 salts; and at ca. 0.025 mol/L for 1:2 and 2:2 salts.

3.2 Charge density of the stationary phase

The stationary phase can be assumed to be a negatively charged hydrogel. The charge in the stationary phase (PPT) is not mobile, and therefore the distribution of ions between the stationary phase and the mobile phase can be examined on the basis of Donnan equilibrium. Electrochemical potentials of a solute both in the stationary phase and in the mobile phase are described as follows

$$\tilde{\mu}_s = \mu_s^\circ + RT \ln a_s + zF\psi + P\overline{v_s} \qquad \text{mobile phase} \tag{2}$$

$$\overline{\tilde{\mu}}_s = \mu_s^\circ + RT \ln \overline{a}_s + zF\overline{\psi} + \overline{P}\overline{v}_s \qquad \text{stationary phase} \tag{3}$$

In addition, the chemical potentials of water in both phases are also explained as follows

$$\tilde{\mu}_w = \mu_w^\circ + RT \ln a_w + P\overline{v}_w \qquad \text{mobile phase} \tag{4}$$

$$\overline{\tilde{\mu}}_w = \mu_w^\circ + RT \ln \overline{a}_w + \overline{P}\overline{v}_w \qquad \text{stationary phase} \tag{5}$$

where $\tilde{\mu}$ is the electrochemical potential, $\mu°$ is the standard electrochemical potential, ψ is the Donnan potential, R is the universal gas constant, F is the Faraday constant, and P is pressure. Symbols with bars denote properties in the stationary phase, and the subscripts "*s*" and "*w*" denote solute and water, respectively.

Because the chemical potentials in both phases are equal under equilibrium conditions, the following equations are obtained

$$\text{Solute}: \quad \tilde{\mu}_s = \bar{\tilde{\mu}}_s, \tag{6}$$

$$\text{Water}: \quad \tilde{\mu}_w = \bar{\tilde{\mu}}_w, \tag{7}$$

$$\Pi = \bar{P} - P = \frac{RT}{\bar{v}_w} \ln \frac{a_w}{\bar{a}_w}, \tag{8}$$

where Π is the swelling pressure. For a 1:1 salt (z = 1), Eq. (6) is rewritten as Eqs. (9) and (10).

$$\tilde{\mu}_+ = \mu_+^\circ + RT \ln a_+ + F\psi + P\bar{v}_+ = \mu_+^\circ + RT \ln \bar{a}_+ + F\bar{\psi} + \bar{P}\bar{v}_+ = \bar{\tilde{\mu}}_+ \quad \text{(cation)} \tag{9}$$

$$\tilde{\mu}_- = \mu_-^\circ + RT \ln a_- - F\psi + P\bar{v}_- = \mu_-^\circ + RT \ln \bar{a}_- + F\bar{\psi} + \bar{P}\bar{v}_- = \bar{\tilde{\mu}}_- \quad \text{(anion)} \tag{10}$$

The Donnan potential based on the cation is described by Eq. (11).

$$\Delta\psi = \bar{\psi} - \psi = \frac{1}{F}\left\{ RT \ln \frac{a_+}{\bar{a}_+} - \left(\bar{P} - P\right)\bar{v}_+ \right\} = \frac{1}{F}\left(RT \ln \frac{a_+}{\bar{a}_+} - \Pi \bar{v}_+ \right) \tag{11}$$

The Donnan potential based on the anion is described by Eq. (12).

$$\Delta\psi = \bar{\psi} - \psi = -\frac{1}{F}\left(RT \ln \frac{a_-}{\bar{a}_-} - \Pi \bar{v}_- \right) \tag{12}$$

Because Eq. (11) is equal to Eq. (12), the following equations can be derived

$$RT \ln \frac{a_+}{\bar{a}_+} - \Pi \bar{v}_+ = -\left(RT \ln \frac{a_-}{\bar{a}_-} - \Pi \bar{v}_- \right) \tag{13a}$$

$$RT \ln \frac{a_+ a_-}{\bar{a}_+ \bar{a}_-} = \Pi\left(\bar{v}_+ + \bar{v}_- \right) \tag{13b}$$

The activity is expressed by the concentration (c) and activity coefficient (γ).

$$c = \gamma a \tag{14}$$

In addition, the effect of swelling pressure can be assumed to be negligible, and therefore the Eq. (15) is derived.

$$\Delta\psi = RT \ln \frac{a_+}{\bar{a}_+} = -RT \ln \frac{\bar{\gamma}_+ \bar{c}_+}{\gamma_+ c_+} = -RT \ln \frac{\lambda_- c_-}{\bar{\gamma}_- \bar{c}_-} \tag{15}$$

$$\gamma_+ c_+ \gamma_- c_- = \bar{\gamma}_+ \bar{c}_+ \bar{\gamma}_- \bar{c}_- \tag{16}$$

Material balance between in the stationary phase and in the bulk solution phase is expressed as follows

$$\bar{c}_+ = X + \bar{c}_-, \qquad \text{(stationary phase)} \tag{17}$$

$$c_+ = c_- = c, \qquad \text{(bulk solution phase)} \tag{18}$$

where X is the charge density of the stationary phase. Substitution of Eqs. (17) and (18) into Eq. (15) gives the concentrations of ions in the stationary phase and the Donnan potential as follows

$$\bar{c}_+ = \left\{ \frac{1}{2}X + \sqrt{\left(\frac{X}{2}\right)^2 + 4c^2 \frac{\gamma_+\gamma_-}{\bar{\gamma}_+\bar{\gamma}_-}} \right\} \tag{19}$$

$$\bar{c}_- = \left\{ -\frac{1}{2}X + \sqrt{\left(\frac{X}{2}\right)^2 + 4c^2 \frac{\gamma_+\gamma_-}{\bar{\gamma}_+\bar{\gamma}_-}} \right\} \tag{20}$$

$$\Delta\psi = -\frac{RT}{F}\ln\left\{ \frac{X}{2c}\frac{\bar{\gamma}_+}{\gamma_+} + \sqrt{\left(\frac{X}{2c}\frac{\bar{\gamma}_+}{\gamma_+}\right)^2 + \frac{\bar{\gamma}_+\gamma_-}{\gamma_+\bar{\gamma}_-}} \right\} \tag{21}$$

Assuming that the solution is a dilute solution and therefore an ideal solution ($\gamma \approx 1$), the Donnan potential ($\Delta\psi$) is approximated by a simpler formula as follows

$$\Delta\psi \approx -\frac{RT}{F}\ln\left\{ \frac{1}{2}\left(\frac{X}{c}\right) + \frac{1}{2}\sqrt{\left(\frac{X}{c}\right)^2 + 1} \right\} \tag{22}$$

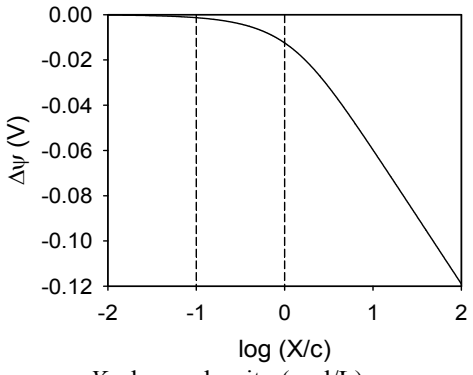

X: charge density (mol/L)
c: salt concentration in bulk phase
$\Delta\psi$: Donnan potential (V)

Fig. 3 Relationship between Donnan potential ($\Delta\psi$) and $\log\left(\frac{X}{c}\right)$

The relationship between $\Delta\psi$ and $\log(X/C)$ is shown in Fig. 3. When X/C is 0.1 ($\log(X/C) = -1$), $\Delta\psi$ is close to zero, and the stationary phase acts like an uncharged material.

When the stationary phase is uncharged, the retention time of the ionic solute is not influenced by solute concentration. Therefore, at an appropriately high salt concentration (i.e., one for which the retention time has plateaued), the charge density of the stationary phase may be evaluated. The average concentration for the 1:1 salts used here was ca. 0.076 mol/L and that for 2:2 salts was ca. 0.036 mol/L. Considering the relationship shown in Fig. 3, the charge density of the stationary phase can be evaluated to be ca. 0.007 eq/L (≈ 7 μeq/g), and this value is considerably lower than the charge density of ion exchange resins for ion chromatography.

When an RO membrane made with the PPT is used for desalination, the charge of the membrane surface contacted with the retentate may be neutralized, but the solute at the outlet side of a pore may be influenced by the charge of the pore wall because of lower salts concentration.

3.3 Adjacent distance of a salt to PPT surface

Even when the charge of the polyamide stationary phase was saturated with cations of a salt, the salt was excluded from the stationary phase because the dielectric constant of PPT, or of the water molecules immediately adjacent to PPT, might have been much lower than that of bulk water, and a large dehydration energy is necessary for a cation to contact PPT. The exclusion of a salt from the PPT surface is a phenomenon similar to the Gibbs' negative adsorption of a salt at the surface of water contacting to air.

The exclusion volume for a salt is calculated as the product of the adjusted retention time and the flow rate of the mobile phase. The exclusion distance of a salt from the PPT surface can be obtained by dividing the exclusion volume by the total surface area of PPT packed in the column. The exclusion distance is considered to be the average adjacent distance between a salt and the PPT surface. The average adjacent distance was calculated by the following equation

$$D = -t_R' \cdot Q/S, \tag{23}$$

where D is the average adjacent distance (m) between a salt and the surface of the stationary phase, t_R' is the adjusted retention time (min), Q is the flow rate (m^3/min) of the mobile phase, and S is the total surface area (m^2) of the stationary phase.

The adjacent distance was calculated for each salt and the average value for each group of salts also was calculated. The average values of the adjacent distances are summarized and presented with their standard deviations in Table 2. It must give useful information to compare the adjacent distance to the pore radius of RO or NF membranes. In our previous work (Kiso *et al*. 2010, 2011), we reported a pore radius of 0.506 nm for an RO membrane (ES10), and pore radii of 0.634 nm and 0.799 nm for two NF membranes (NTR-729HF and NTR-725, respectively). These pore radii were obtained by approximating the shape of an organic molecule to be a rectangular parallelepiped. The average adjacent distance obtained for the 1:1 salts was close to the pore radius of the ES10 RO membrane, and that obtained for the 2:2 salts was close to the pore radius of the NTR-729HF NF membrane. However, we note that these parameters, i.e., the average distance and pore radii measurements, were obtained by quite different approaches.

The adjacent distances may be related to the hydration radius or hydration energy of the ion, and Tansel (2012) discussed the effects of these parameters on membrane separation. In membrane separation, the average adjacent distance may serve an important role at the pore inlet side

Table 2 Adjacent distance (nm) of salts to the stationary phase

salt	Average distance (nm)	Standard deviation (nm)	remark
1:1	0.49	0.069	**
2:1	0.57	0.060	**
1:2	0.60	0.085	**
2:2	0.66	0.030	**

**: significant at 0.05 of significance level

(retentate side), and this can be considered a sieving effect, whereas the driving force is electrochemical interaction. On the other hand, the salt concentration inside a pore may be lower than that of the retentate, and therefore the repulsive intensity for ions may increase, as was observed in the data shown in Figs. 1 and 3. These results indicate that the transport of ions in a pore should be considered the effect of surface charge of pore wall.

3.4 Retained salts in the stationary phase

There are some inorganic compounds that are not effectively rejected, even by RO membranes; such compounds include arsenite (As(III)), boron, and $HgCl_2$. The interaction of these compounds with the PPT stationary phase was also examined in this study. Solutions of $NaAsO_2$, H_3BO_3 or $HgCl_2$ were prepared at concentrations in the range of 0.005-0.1 mol/L. The plots of the retention time versus injected concentration of these salts are presented in Fig. 4. For these experiments, the concentrations at the surface of the stationary phase were not evaluated but can be expected to be 3%-10% of the injected concentration.

These three compounds showed different retention behavior. The retention times of H_3BO_3 were almost constant and close to t_0 for the entire concentration range tested. $NaAsO_2$ was retained slightly over the entire concentration range. $HgCl_2$ was rejected at low concentrations (< 0.04 mol/L), and its retention time increased asymptotically to t_0 with increasing injected concentration.

Both H_3AsO_3 and H_3BO_3 are weak acids, and the pK_1 of these species were 9.2 and 9.24, respectively. Therefore, at neutral pH, the major species of each compound is its undissociated form, and therefore the rejection of these compounds by a membrane may be controlled only by the molecular sieving effect. The fact that the molecular sizes of these compounds are much smaller than glucose may explain the low rejection degrees for these compounds.

When cellulose acetate was used stationary phase, $HgCl_2$ was retained by the column (Kiso *et al*. 1996b). However, in the case of PPT column, $HgCl_2$ was slightly rejected. $HgCl_2$ as well as boric acid dissolved as undissociated species. The concentrations of chemical species in aqueous $HgCl_2$ solution system were calculated on the basis of the equilibrium equations (Hepler and Olofsson 1975).

$$HgCl^+(aq) + Cl^-(aq) = HgCl_2(aq) \qquad K_1 = 2.5\times10^6$$
$$Hg^{2+}(aq) + Cl^-(aq) = HgCl^+(aq) \qquad K_2 = 5.8\times10^6$$
$$HgCl_2(aq) + OH^-(aq) = HgCl(OH)(aq) + Cl^-(aq) \qquad K_3 = 1.2\times10^4$$
$$HgCl_2(aq) + 2OH^-(aq) = Hg(OH)_2(aq) + 2Cl^-(aq) \qquad K_4 = 5\times10^8$$

The relationship between the part of the non-ionic species ($HgCl_2$(aq) + HgCl(OH)(aq) +

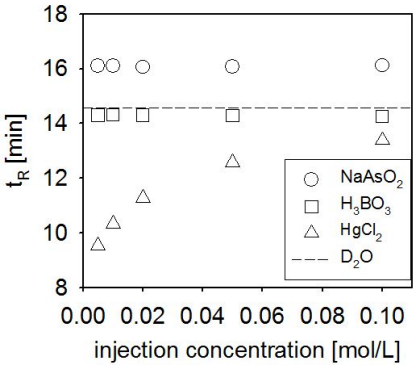

Fig. 4 Plots of retention time versus concentration of injected solution

$Hg(OH)_2(aq)$) and total mercury concentration is shown in Fig. 5. The part of ionic species increased slightly only in the region of very low total mercury concentration, and the results are not sufficient evidence for the chromatographic behavior of $HgCl_2$ shown in Fig. 4. The repulsive interaction between $HgCl_2$ and PPT stationary phase is a future subject.

4. Conclusions

The interaction between inorganic salts and PPT, which is a material similar to the skin layer of polyamide membranes, was examined by an inverse HPLC method. Salts were excluded from the PPT surface, and the exclusion intensity was influenced by the concentration and valence of the ions. The retention properties and the results of potential measurements indicate that PPT was slightly negatively charged. When the surface charge of PPT was saturated, the exclusion intensity increased in the order of 1:1 < 2:1 < 1:2 ≈ 2:2 salts, and the average exclusion distance (average adjacent distance between the salt and the stationary phase) varied in the range from ca. 0.49 nm (1:1 salt) to 0.66 nm (2:2 salt). The values were close to the pore radii of RO and NF membranes obtained by numerical simulation.

As(III) and boron, which are rejected poorly even by RO membranes, were not excluded effectively from the PPT stationary phase, and these results might have been caused by the fact that the compounds are dissolved in their undissociated forms in the neutral-pH aqueous solution system used here.

Acknowledgments

This work was financially supported by the Research Project on Development of Innovative Membrane Separation Technology, sponsored by the New Energy and Industrial Technology Development Organization (NEDO) of Japan.

References

Bellona, C. and Drewes, J.E. (2005), “The role of membrane surface charge and solute physico-chemical

properties in the rejection of organic acids by NF membranes", *J. Membr. Sci*., **249**(1-2), 227-234.
Bowen, W.R. and Welfoot, J.S. (2002a), "Modeling of the performance of membrane nanofiltration−critical assessment and model development", *Chem. Eng. Sci*., **57**(7), 1121-1137.
Bowen, W.R. and Welfoot, J.S. (2002b), "Modeling of membrane nanofiltration−pore size distribution effects", *Chem. Eng. Sci*., **57**(8), 1393-1407.
Bruggen, B.V.D., Vandecasteele, C., Gestel, T.V., Doyen, W. and Leysen, R. (2003), "A review of pressure-driven membrane processes in wastewater treatment and drinking water production", *Environ. Progr*., **22**(1), 46-56.
Comerton, A.M., Andrews, R.C., Bagley, D.M. and Yang, P. (2007), "Membrane adsorption of endocrine disrupting compounds and pharmaceutically active compounds", *J. Membr. Sci*., **303**(1-2), 267-277.
David, A.B., Bason, S., Jopp, J., Oren, Y. and Freger, V. (2006), "Partitioning of organic solutes between water and polyamide layer of RO and NF membranes: Correlation to rejection", *J. Membr. Sci*., **281**(1-2), 480-490.
Déon, S., Dutournié, P., Limousy, L. and Bourseau, P. (2009), "Transport of salt mixtures through nanofiltration membranes: Numerical identification of electric and dielectric contributions", *Sep. Purif. Technol*., **69**(3), 225-233.
Dolar, D., Pelko, S., Košutić, K.A. and Horvat, J.M. (2012), "Removal of anthelmintic drugs and their photodegradation products from water with RO/NF membranes", *Process Saf. Environ. Protect*., **90**(2), 147-152.
Ghaffour, N., Missimer, T.M. and Amy, G.L. (2013), "Technical review and evaluation of the economics of water desalination: Current and future challenges for better water supply sustainability", *Desalination*, **309**, 197-207.
Hepler, L.G. and Olofsson, G. (1975), "Mercury. Thermodynamic properties, chemical equilibriums, and standard potentials", *Chem. Rev*., **75**(5), 585-602.
Jung, Y.J., Kiso, Y., Othman, R.A.A., Ikeda, A., Min, K.S., Kumano, A. and Ariji, A. (2005), "Rejection properties of aromatic pesticides with a hollow fiber NF membrane", *Desalination*, **180**(1-3), 63-71.
Kimura, K., Amy, G., Drewes, J. and Watanabe, Y. (2003a), "Adsorption of hydrophobic compounds onto NF/RO membranes: an artifact leading to overestimation of rejection", *J. Membr. Sci*., **221**(1-2), 89-101.
Kimura, K., Amy, G., Drewes, J.E., Heberer, T., Kim, T.U. and Watanabe, Y. (2003b), "Rejection of organic micropollutants (disinfection by-products, endocrine disrupting compounds, and pharmaceutically active compounds) by NF/RO membranes", *J. Membr. Sci*., **227**(1-2), 113-121.
Kiso, Y. (1986), "Factors affecting adsorption of organic solutes on cellulose acetate in an aqueous solution system", *Chromatographia*, **22**(1-6), 55-58
Kiso, Y. and Kitao, T. (1986), "Elution characteristics of polymeric solutes and inorganic salts in HPLC on a cellulose acetate column", *Chromatographia*, **22**(7-12), 341-344.
Kiso, Y., Kitao, T., Ge, Y.S. and Jinno, K. (1989), "Retention characteristics of aliphatic compounds on ellulose acetate as a stationary phase with an aqueous mobile phase", *Chromatographia*, **28**(5-6), 279-284.
Kiso, Y., Kitao, T. and Nishimura, K. (1999a), "Adsorption properties of cyclic compounds on cellulose acetate", *J. Appl. Polym. Sci*., **71**(10), 1657-1664.
Kiso, Y., Kitao, T. and Nishimura, K. (1999b), "Adsorption properties of aromatic compounds on polyethylene as a ‚embrane material", *J. Appl. Polym. Sci*., **74**(5), 1037-1043.
Kiso, Y., Kon, T. Kitao, T. and Nishimura, K. (2001a), "Rejection properties of alkyl phthalates with nanofiltration membranes", *J. Membrane Sci*., **182**(1-2), 205-214.
Kiso, Y., Sugiura, Y., Kitao, T. and Nishimura, K. (2001b), "Effects of hydrophobicity and molecular size on rejection of aromatic pesticides with nanofiltration membranes", *J. Membr. Sci*., **192**(1-2), 1-10.
Kiso, Y., Muroshige, K., Oguchi, T., Yamada, T., Hirose, M., Ohara, T. and Shintani, T. (2010), "Effect of molecular shape on the rejection of uncharged organic compounds by nanofiltration membranes and on calculated pore radii", *J. Membr. Sci*., **358**(1-2), 101-113.
Kiso, Y., Muroshige, K., Oguchi, T., Hirose, M., Ohara, T. and Shintani, T. (2011), "Pore radius estimation based on organic solute molecular shape and effects of pressure on pore radius for a reverse osmosis

membrane", *J. Membr. Sci.*, **369**(1-2), 290-298.
Kiso, Y., Hosogi, K., Kamimoto, Y. and Jung, Y.J. (2014), "Evaluation of interaction between organic solutes and a membrane polymer by an inverse HPLC method", *Membr. Water Treat., Int. J.*, **5**(3), 171-182.
Lint, W.B.S. and Benes, N.E. (2004), "Predictive charge-regulation transport model for nanofiltration from the theory of irreversible processes", *J. Membr. Sci.*, **243**(1-2), 365-377.
Malaisamy, R., Talla-Nwafo A. and Jones, K.L. (2011), "Polyelectrolyte modification of nanofiltration membrane for selective removal of monovalent anions", *Sep. Purif. Technol.*, **77**(3), 367-374.
Plakas, K.V. and Karabelas, A.J. (2012), "Removal of pesticides from water by NF and RO membranes — A review", *Desalination*, **287**, 255-265.
Semião, A.J.C. and Schäfer, A.I. (2013), "Removal of adsorbing estrogenic micropollutants by nanofiltration membranes. Part A-Experimental evidence", *J. Membr. Sci.*, **431**, 244-256.
Schaep, J. and Vandecasteele, C. (2001), "Evaluating the charge of nanofiltration membranes", *J. Membr. Sci.*, **188**(1), 129-136.
Szymczyk, A. and Fievet, P. (2005), "Investigating transport properties of nanofiltration membranes by means of a steric, electric and dielectric exclusion model", *J. Membr. Sci.*, **252**(1-2), 77-88.
Tansel, B. (2012), "Significance of thermodynamic and physical characteristics on permeation of ions during membrane separation: Hydrated radius, hydration free energy and viscous effects", *Sep. Purif. Technol.*, **86**, 119-126.
Verliefde, A.R.D., Cornelissen, E.R., Heijman,S.G.J., Verberk, J.Q.J.C., Amy, G.L., Bruggen, B.V. and Dijk, J.C. (2008), "The role of electrostatic interactions on the rejection of organic solutes in aqueous solutions with nanofiltration", *J. Membr. Sci.*, **322**(1), 52-66.
Wang, X.-L., Tsuru, T., Togoh, M., Nakano, S. and Kimura, S. (1995), "Evaluation of pore structure and electrical properties of nanofiltration membranes", *J. Chem. Eng, Jpn.*, **28**(2), 186-192.
Wang, X.-L., Tsuru, T., Nakao, S. and Kimura, S. (1997), "The electrostatic and steric-hindrance model for the transport of charged solutes through nanofiltration membranes", *J. Membr. Sci.*, **135**(1), 19-32.
Yaroshchuk, A.E. (2001), "Non-steric mechanisms of nanofiltration: Superposition of Donnan and dielectric exclusion", *Sep. Purif. Technol.*, **22-23**, 143-158.

ED

Symbol

a	activity
c	concentration
F	Faraday constant
P	Pressure
R	universal gas constant
$\bar{v}$	partial molar volume
X	charge density of membrane
γ	activity coefficient
$\tilde{\mu}$	electrochemical potential
μ°	standard electrochemical potential
ψ	Donnan potential

Suffix

+	cation
−	anion
w	water